Theory of prismatic folded plate structures

Autor(en): **Goldberg, John E. / Leve, Howard L.**

Objekttyp: **Article**

Zeitschrift: **IABSE publications = Mémoires AIPC = IVBH Abhandlungen**

Band (Jahr): **17 (1957)**

PDF erstellt am: **23.04.2024**

Persistenter Link: https://doi.org/10.5169/seals-15754

Theory of Prismatic Folded Plate Structures

Théorie des systèmes de parois prismatiques

Theorie der prismatischen Faltwerke

JOHN E. GOLDBERG, Ph. D., Professor of Structural Engineering, Purdue University, Lafayette, Indiana, U.S.A., and

HOWARD L. LEVE, Ph. D., Engineer, Douglas Aircraft Company, Santa Monica, California, U.S.A., formerly Graduate Student, Purdue University

Introduction

During recent years folded plate construction has found increasing application for roofs of industrial buildings and hangars as well as for the sides and bottoms of elevated bunkers. Such construction is particularly well-suited to fairly long spans, possessing some of the attributes of thin shell construction with, perhaps, the added advantage of somewhat simpler fabrication or forming.

The folded plate structure is a prismoidal shell formed by a series of adjoining thin plane slabs rigidly connected along their common edges, ane usually closed off at its ends by integral diaphragms. This type of structurd is generally of reinforced concrete and may be illustrated by fig. 1. More complicated configurations are possible. The folded plate structure may have any

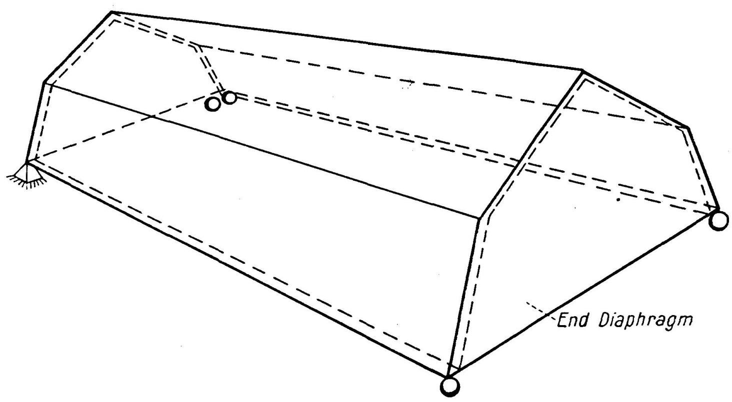

Fig. 1. Folded Plate Structure.

number of slabs meeting at the joints, and it may be non-prismatic. The structure also may be continuous in the longitudinal direction over several diaphragms or supports.

A theory of folded plate structures appears to have been developed first by G. Ehlers [1], who used a membrane solution assuming negligible displacements of the joints. This membrane approach considered the slabs as beams supported at the end diaphragms and hence with a linear stress distribution across their widths. Subsequently E. Gruber [4], using a strip theory approach, was able to take approximate account of joint translations and rotations. A further refinement in the membrane theory, by H. Craemer [12] and E. Gruber [18] considered the actual stress distributions in the planes of the slabs. The latter papers used Airy's stress function to obtain the planar stress distribution, instead of assuming an elementary beam theory. Recently, A. Werfel [19] indicated an approach which considers both elasticity and plate action of the slabs and requires satisfying equilibrium and compatibility equations at the joints. Werfel's approach essentially requires the solving of $8n$ simultaneous equations, where n is the number of joints with unknown forces and displacements.

J. E. Goldberg has outlined the following formulation which considers the simultaneous plate bending and membrane action of the several slabs and yields a solution involving tabulated functions. The forces at the longitudinal edges of each slab are expressed as fixed-edge forces corrected or modified by the effect of displacement of the joints. These displacements are visualized as being four in number at each point of the joint; two components of translation and a rotation, all lying in the plane normal to the joint, and a translation in the direction of the joint. It is assumed that the joint displacements can be expanded into Fourier half-range series. At each longitudinal edge of a slab, four distributed generalized forces will exist; namely, a force in the plane of the slab and normal to its edge, a shear in the direction of the thickness, a longitudinal shear, and an edge moment. Each of these distributed generalized forces is linearly dependent upon the four components of displacement at both edges of the slab, and may also be expanded into Fourier series. The relation between the four generalized edge forces and the displacements is determined *a priori* by a semi-inverse technique which is essentially typical for each component. An arbitrary harmonic of one of the displacements is applied to one edge of the slab and the resulting homogeneous boundary value problem is solved for the displacements within the slab. These displacements define the resulting forces in the interior of the slab and, in particular, they establish the forces at each edge due to the element of displacement at one edge. These *edge-force / edge-displacement* relations are used in writing the joint equilibrium equations, as well as in evaluating the fixed edge forces of the loaded slabs.

The purpose of this paper is to present and illustrate the last-mentioned classical theory for prismatic folded plate structures. This theory incorporates the usual assumptions of plate and elasticity theory plus the restrictions that no displacements are permitted in the planes of the end diaphragms and no resistance is offered normal to these planes.

It is necessary, in a classical approach, to use elasticity theory for displacements in the plane of the slab, since in many structures, such as bunkers, the slabs have small length to width ratios and the assumption of a linear stress distribution across each slab may be considerably in error. However, the use of Airy's stress function for the solution of the elasticity problem is awkward and in this paper a semi-inverse approach will be used as formulated by the senior author.

Since, in general, the membrane forces acting upon a joint are not collinear, plate shears are necessary to place the joint in equilibrium as can be seen in fig. 2. It follows that both plate theory and two-dimensional elasticity theory are required in the classical solution of a folded plate structure.

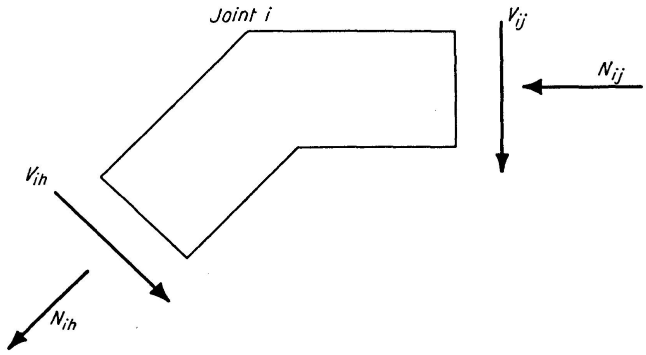

Fig. 2. Edge Forces Acting on a Joint.

In this paper, the joint forces are expressed in terms of the joint displacements as in the slope deflection method, thus eliminating the use of differential equations. It is then only necessary to solve $4n$ simultaneous algebraic equations, where n is the number of joints with unknown forces and displacements, for each harmonic of the Fourier expansion. Only routine calculations and tabulated functions are involved in the writing of these equations.

The derivation of the necessary formulas is presented in the sections immediately following. In using the method, however, one need not be completely familiar with the details of the derivation. A numerical example is included to illustrate the method.

Edge Displacement. Force Relations for Slabs

Before deriving the equations for the complete structure, we consider an individual slab and we develop formulas for the internal forces resulting from the various generalized edge displacements. These edge displacements are of two types, namely, displacements normal to the slab and displacements in the plane of the slab. The former involve plate theory while the latter involve two-dimensional elasticity theory. We first treat the displacements normal to the slab. Symbols and sign convention are defined in Appendix A.

I. Displacements Normal to the Slab

The normal displacements may be expanded into the Fourier series:

$$w(x,y) = \Sigma W_m(y) \sin\frac{m\pi x}{a}. \tag{1}$$

If we now admit only the mth term, then the deflections $w_m = W_m(y)\sin\frac{m\pi x}{a}$ must satisfy the homogeneous differential equation

$$\frac{\partial^4 w_m}{\partial x^4} + 2\frac{\partial^4 w_m}{\partial x^2 \partial y^2} + \frac{\partial^4 w_m}{\partial y^4} = 0. \tag{2}$$

For w_m to satisfy eq. (2), $W_m(y)$ must be of the form

$$W_m = A_{1m}\sinh\frac{m\pi y}{a} + A_{2m}\cosh\frac{m\pi y}{a} + A_{3m}\frac{m\pi y}{a}\sinh\frac{m\pi y}{a} + A_{4m}\frac{m\pi y}{a}\cosh\frac{m\pi y}{a}.$$

The plate problem may now be resolved into the following two edge displacement cases for a typical slab $i-j$.

Case A. Rotations of Edges i and j. The boundary conditions for this case are taken to be the following:

$$w_m = 0 \text{ and } \frac{\partial^2 w_m}{\partial x^2} = 0 \text{ for } x=0 \text{ and } x=a, \tag{3}$$

$$w_m = 0 \text{ for } y = \pm\frac{b}{2}, \tag{4}$$

$$\left(\frac{\partial w_m}{\partial y}\right)_{y=b/2} = \bar{\theta}_{im}\sin\frac{m\pi x}{a}; \quad \left(\frac{\partial w_m}{\partial y}\right)_{y=-b/2} = \bar{\theta}_{jm}\sin\frac{m\pi x}{a}. \tag{5}$$

It can be seen that the expression for w_m satisfies boundary condition (3).

The discussion can now be simplified by separation into two particular cases:

1. The symmetrical case in which $\left(\frac{\partial w_m}{\partial y}\right)_{y=b/2} = -\left(\frac{\partial w_m}{\partial y}\right)_{y=-b/2}$.
2. The anti-symmetrical case in which $\left(\frac{\partial w_m}{\partial y}\right)_{y=b/2} = \left(\frac{\partial w_m}{\partial y}\right)_{y=-b/2}$.

In the symmetrical case W_m must be an even function of y, and hence $A_{1m} = A_{4m} = 0$.

In satisfying boundary conditions (4), we find that

$$A_{2m} = -A_{3m}\alpha_m \tanh\alpha_m, \text{ where } \alpha_m = \frac{m\pi b}{2a}.$$

Hence we now have

$$w_m = A_{3m}\left(\frac{m\pi y}{a}\sinh\frac{m\pi y}{a} - \alpha_m \tanh\alpha_m \cosh\frac{m\pi y}{a}\right)\sin\frac{m\pi x}{a}. \tag{6}$$

For the symmetrical case, the rotations along the edges $y = \pm\frac{b}{2}$ are taken to be

$$\theta'_{im}(x) = -\theta'_{jm}(x) = \bar{\theta}'_{im}\sin\frac{m\pi x}{a},$$

where the "primes" refer to the symmetrical case.

From boundary condition (5) it then follows that

$$A_{3m} = \frac{a\,\bar{\theta}'_{im}}{m\pi(\alpha_m \operatorname{sech}\alpha_m + \sinh\alpha_m)}.$$

Substituting this result into eq. (6), we obtain for the symmetrical case:

$$w_m = \frac{a}{m\pi}\frac{\bar{\theta}'_{im}\sin\frac{m\pi x}{a}}{(\alpha_m \operatorname{sech}\alpha_m + \sinh\alpha_m)}\left(\frac{m\pi y}{a}\sinh\frac{m\pi y}{a} - \alpha_m\tanh\alpha_m\cosh\frac{m\pi y}{a}\right). \tag{7}$$

For the anti-symmetrical case, W_m must be an odd function of y. Hence $A_{2m} = A_{3m} = 0$.

Boundary condition (4) requires that

$$A_{1m} = -A_{4m}\,\alpha_m \coth\alpha_m.$$

Hence we now have

$$w_m = A_{4m}\left(\frac{m\pi y}{a}\cosh\frac{m\pi y}{a} - \alpha_m\coth\alpha_m\sinh\frac{m\pi y}{a}\right)\sin\frac{m\pi x}{a}. \tag{8}$$

For the anti-symmetrical case, the rotations along the edges $y = \pm\frac{b}{2}$ are as follows:

$$\theta''_{im}(x) = \theta''_{jm}(x) = \bar{\theta}''_{im}\sin\frac{m\pi x}{a},$$

where the "double primes" refer to the anti-symmetrical case.

From boundary condition (5) we find A_{4m}.

Substituting this value for A_{4m} into eq. (8) we finally get for the anti-symmetrical case

$$w_m = -\frac{a}{m\pi}\frac{\bar{\theta}''_{im}\sin\frac{m\pi x}{a}}{(\alpha_m \operatorname{csch}\alpha_m - \cosh\alpha_m)}\left(\frac{m\pi y}{a}\cosh\frac{m\pi y}{a} - \alpha_m\coth\alpha_m\sinh\frac{m\pi y}{a}\right). \tag{9}$$

Since the amplitude of rotation at edge i is $\bar{\theta}_{im}$ and at edge j, $\bar{\theta}_{jm}$, then the symmetrical part is

$$\bar{\theta}'_{im} = \tfrac{1}{2}(\bar{\theta}_{im} - \bar{\theta}_{jm}) \tag{10}$$

and the anti-symmetrical part is

$$\bar{\theta}''_{im} = \tfrac{1}{2}(\bar{\theta}_{im} + \bar{\theta}_{jm}). \tag{11}$$

Hence adding the symmetrical and anti-symmetrical parts for w_m and using relations (10) and (11), we obtain for this case

$$\begin{aligned} w_m = \tfrac{1}{2} s_{-1m}(x) \,\big[&\bar{\theta}_{im}\{\lambda_{1m}[S_{1m}(y) - k_{tm} C_m(y)] - \lambda_{2m}[C_{1m}(y) - k_{cm} S_m(y)]\} \\ &- \bar{\theta}_{jm}\{\lambda_{1m}[S_{1m}(y) - k_{tm} C_m(y)] + \lambda_{2m}[C_{1m}(y) - k_{cm} S_m(y)]\}\big] \end{aligned} \tag{12}$$

where

$$\lambda_{1m} = (\alpha_m \operatorname{sech}\alpha_m + \sinh\alpha_m)^{-1}; \qquad \lambda_{2m} = (\alpha_m \operatorname{csch}\alpha_m - \cosh\alpha_m)^{-1};$$

$$k_{tm} = \alpha_m \tanh\alpha_m; \qquad k_{cm} = \alpha_m \coth\alpha_m; \qquad s_{-1m}(x) = \frac{a}{m\pi}\sin\frac{m\pi x}{a};$$

$$S_m(y) = \sinh\frac{m\pi y}{a}; \qquad C_m(y) = \cosh\frac{m\pi y}{a};$$

$$S_{1m}(y) = \frac{m\pi y}{a}\sinh\frac{m\pi y}{a}; \qquad C_{1m}(y) = \frac{m\pi y}{a}\cosh\frac{m\pi y}{a}.$$

Using eq. (12), we calculate the following expressions for the forces:

$$\begin{aligned} M_{ym} &= -D\left(\frac{\partial^2 w_m}{\partial y^2} + \nu\frac{\partial^2 w_m}{\partial x^2}\right) \\ &= D_1 s_{1m}(x)\,\big[\bar{\theta}_{im}\{-\lambda_{1m}[S_{1m}(y)+(\mu_1-k_{tm})C_m(y)]+\lambda_{2m}[C_{1m}(y)+(\mu_1-k_{cm})S_m(y)]\} \\ &\qquad + \bar{\theta}_{jm}\{\ \lambda_{1m}[S_{1m}(y)+(\mu_1-k_{tm})C_m(y)]+\lambda_{2m}[C_{1m}(y)+(\mu_1-k_{cm})S_m(y)]\}\big], \end{aligned} \tag{13}$$

$$\begin{aligned} M_{xm} &= -D\left(\frac{\partial^2 w_m}{\partial x^2} + \nu\frac{\partial^2 w_m}{\partial y^2}\right) \\ &= D_1 s_{1m}(x)\,\big[\bar{\theta}_{im}\{\lambda_{1m}[S_{1m}(y)-(\mu_2+k_{tm})C_m(y)]-\lambda_{2m}[C_{1m}(y)-(\mu_2+k_{cm})S_m(y)]\} \\ &\qquad - \bar{\theta}_{jm}\{\lambda_{1m}[S_{1m}(y)-(\mu_2+k_{tm})C_m(y)]+\lambda_{2m}[C_{1m}(y)-(\mu_2+k_{cm})S_m(y)]\}\big], \end{aligned} \tag{14}$$

$$\begin{aligned} Q_{ym} &= -D\left(\frac{\partial^3 w_m}{\partial y^3} + \frac{\partial^3 w_m}{\partial y\,\partial x^2}\right) \\ &= D s_{2m}(x)\{\bar{\theta}_{im}[-\lambda_{1m} S_m(y) + \lambda_{2m} C_m(y)] + \bar{\theta}_{jm}[\lambda_{1m} S_m(y) + \lambda_{2m} C_m(y)]\}, \end{aligned} \tag{15}$$

$$\begin{aligned} Q_{xm} &= -D\left(\frac{\partial^3 w_m}{\partial x^3} + \frac{\partial^3 w_m}{\partial x\,\partial y^2}\right) \\ &= D c_{2m}(x)\{\bar{\theta}_{im}[-\lambda_{1m} C_m(y) + \lambda_{2m} S_m(y)] + \bar{\theta}_{jm}[\lambda_{1m} C_m(y) + \lambda_{2m} S_m(y)]\}, \end{aligned} \tag{16}$$

$$\begin{aligned} M_{yxm} &= -M_{xym} = -D(1-\nu)\frac{\partial^2 w_m}{\partial x\,\partial y} \\ &= D_1 c_{1m}(x)\,\big[\bar{\theta}_{im}\{-\lambda_{1m}[C_{1m}(y)+(1-k_{tm})S_m(y)]+\lambda_{2m}[S_{1m}(y)+(1-k_{cm})C_m(y)]\} \\ &\qquad + \bar{\theta}_{jm}\{\ \lambda_{1m}[C_{1m}(y)+(1-k_{tm})S_m(y)]+\lambda_{2m}[S_{1m}(y)+(1-k_{cm})C_m(y)]\}\big], \end{aligned} \tag{17}$$

where

$$s_{1m}(x) = \frac{m\pi}{a}\sin\frac{m\pi x}{a}; \qquad s_{2m}(x) = \frac{m^2\pi^2}{a^2}\sin\frac{m\pi x}{a};$$

$$c_{1m}(x) = \frac{m\pi}{a}\cos\frac{m\pi x}{a}; \qquad c_{2m}(x) = \frac{m^2\pi^2}{a^2}\cos\frac{m\pi x}{a};$$

$$D = \frac{E h^3}{12(1-\nu^2)}; \qquad D_1 = \frac{E h^3}{24(1+\nu)};$$

$$\mu_1 = \frac{2}{1-\nu}; \qquad \mu_2 = \frac{2\nu}{1-\nu}.$$

Case B. Translations of Edges i and j. The boundary conditions for this case are

$$w_m = 0 \text{ and } \frac{\partial^2 w_m}{\partial x^2} = 0 \text{ for } x = 0 \text{ and } x = a, \tag{18}$$

$$\frac{\partial w_m}{\partial y} = 0 \text{ for } y = \pm\frac{b}{2}, \tag{19}$$

$$(w_m)_{y=b/2} = \overline{w}_{ijm} \sin\frac{m\pi x}{a}; \qquad (w_m)_{y=-b/2} = \overline{w}_{jim} \sin\frac{m\pi x}{a}. \tag{20}$$

For simplification, the solution for w_m can again be separated into a symmetrical and anti-symmetrical part, which requires the use of only two arbitrary constants for each part. The two constants, as before, are determined from boundary conditions (19) and (20). The symmetrical and anti-symmetrical parts are then combined to give the complete solution for w_m.

Hence we get for this case, using the symbols in case I A,

$$\begin{aligned} w_m = {} & \tag{21} \\ & \tfrac{1}{2} s_m(x) \big[\overline{w}_{ijm}\{-\lambda_{3m}[S_{1m}(y)-(1+k_{cm})\,C_m(y)]+\lambda_{4m}[C_{1m}(y)-(1+k_{tm})\,S_m(y)]\} \\ & \quad -\overline{w}_{jim}\{\ \lambda_{3m}[S_{1m}(y)-(1+k_{cm})\,C_m(y)]+\lambda_{4m}[C_{1m}(y)-(1+k_{tm})\,S_m(y)]\}\big], \end{aligned}$$

where

$$\lambda_{3m} = (\alpha_m \operatorname{csch}\alpha_m + \cosh\alpha_m)^{-1}; \qquad \lambda_{4m} = (\alpha_m \operatorname{sech}\alpha_m - \sinh\alpha_m)^{-1};$$

$$s_m(x) = \sin\frac{m\pi x}{a}.$$

From eq. (21), we get the following expressions for the forces:

$$\begin{aligned} M_{ym} = {} & \tag{22} \\ & D_1 s_{2m}(x) \big[\overline{w}_{ijm}\{\lambda_{3m}[S_{1m}(y)+(\mu_3-k_{cm})\,C_m(y)]-\lambda_{4m}[C_{1m}(y)+(\mu_3-k_{tm})\,S_m(y)]\} \\ & \quad +\overline{w}_{jim}\{\lambda_{3m}[S_{1m}(y)+(\mu_3-k_{cm})\,C_m(y)]+\lambda_{4m}[C_{1m}(y)+(\mu_3-k_{tm})\,S_m(y)]\}\big], \end{aligned}$$

$$\begin{aligned} M_{xm} = {} & \tag{23} \\ & D_1 s_{2m}(x) \big[\overline{w}_{ijm}\{-\lambda_{3m}[S_{1m}(y)-(\mu_3+k_{cm})\,C_m(y)]+\lambda_{4m}[C_{1m}(y)-(\mu_3+k_{tm})\,S_m(y)]\} \\ & \quad -\overline{w}_{jim}\{\ \lambda_{3m}[S_{1m}(y)-(\mu_3+k_{cm})\,C_m(y)]+\lambda_{4m}[C_{1m}(y)-(\mu_3+k_{tm})\,S_m(y)]\}\big], \end{aligned}$$

$$Q_{ym} = D s_{3m}(x)\{\overline{w}_{ijm}[\lambda_{3m} S_m(y)-\lambda_{4m} C_m(y)]+\overline{w}_{jim}[\lambda_{3m} S_m(y)+\lambda_{4m} C_m(y)]\}, \tag{24}$$

$$Q_{xm} = D c_{3m}(x)\{\overline{w}_{ijm}[\lambda_{3m} C_m(y)-\lambda_{4m} S_m(y)]+\overline{w}_{jim}[\lambda_{3m} C_m(y)+\lambda_{4m} S_m(y)]\}, \tag{25}$$

$$\begin{aligned} M_{yxm} = {} & D_1 c_{2m}(x) \big[\overline{w}_{ijm}\{\lambda_{3m}[C_{1m}(y)-k_{cm} S_m(y)]-\lambda_{4m}[S_{1m}(y)-k_{tm} C_m(y)]\} \\ & \quad +\overline{w}_{jim}\{\lambda_{3m}[C_{1m}(y)-k_{cm} S_m(y)]+\lambda_{4m}[S_{1m}(y)-k_{tm} C_m(y)]\}\big], \end{aligned} \tag{26}$$

where

$$s_{3m}(x) = \frac{m^3\pi^3}{a^3}\sin\frac{m\pi x}{a}; \qquad c_{3m}(x) = \frac{m^3\pi^3}{a^3}\cos\frac{m\pi x}{a}; \qquad \mu_3 = \frac{1+\nu}{1-\nu}.$$

II. Displacements in the Plane of the Slab:

The governing differential equations involving this type of displacements may be obtained in the following manner:

Let us take

$$u_m(x,y) = U_m(y)\cos\frac{m\pi x}{a}, \tag{27}$$

$$v_m(x,y) = V_m(y)\sin\frac{m\pi x}{a}. \tag{28}$$

Then we get the following expressions for the stresses:

$$\begin{aligned}
\sigma_{xm} &= \frac{E}{1-\nu^2}\left(\frac{\partial u_m}{\partial x}+\nu\frac{\partial v_m}{\partial y}\right) = \frac{E}{1-\nu^2}\left(-\frac{m\pi}{a}U_m+\nu\frac{dV_m}{dy}\right)\sin\frac{m\pi x}{a},\\
\sigma_{ym} &= \frac{E}{1-\nu^2}\left(\frac{\partial v_m}{\partial y}+\nu\frac{\partial u_m}{\partial x}\right) = \frac{E}{1-\nu^2}\left(\frac{dV_m}{dy}-\frac{m\pi}{a}\nu U_m\right)\sin\frac{m\pi x}{a},\\
\tau_{xym} &= G\left(\frac{\partial u_m}{\partial y}+\frac{\partial v_m}{\partial x}\right) = \frac{E}{2(1+\nu)}\left(\frac{dU_m}{dy}+\frac{m\pi}{a}V_m\right)\cos\frac{m\pi x}{a}.
\end{aligned} \tag{29}$$

Substituting the above expressions for the stresses into the two equilibrium equations:

$$\frac{\partial\sigma_{xm}}{\partial x}+\frac{\partial\tau_{xym}}{\partial y} = 0 \quad\text{and}\quad \frac{\partial\sigma_{ym}}{\partial y}+\frac{\partial\tau_{xym}}{\partial x} = 0,$$

we arrive at the following governing equations:

$$\frac{E}{2(1+\nu)}\left\{\left[D^2-\frac{2}{(1-\nu)}\left(\frac{m\pi}{a}\right)^2\right]U_m+\left[\frac{1+\nu}{1-\nu}\frac{m\pi}{a}D\right]V_m\right\}\cos\frac{m\pi x}{a} = 0, \tag{30}$$

$$\frac{E}{2(1+\nu)}\left\{-\left[\frac{1+\nu}{1-\nu}\frac{m\pi}{a}D\right]U_m+\left[\frac{2}{1-\nu}D^2-\left(\frac{m\pi}{a}\right)^2\right]V_m\right\}\sin\frac{m\pi x}{a} = 0, \tag{31}$$

where $D = \frac{d}{dy}$ and $D^2 = \frac{d^2}{dy^2}$.

It can be readily verified that the values of U_m and V_m satisfying these two differential equations are as follows:

$$\begin{aligned}
U_m = A_{1m}\cosh\frac{m\pi y}{a}+A_{2m}\sinh\frac{m\pi y}{a}+A_{3m}\frac{m\pi y}{a}\cosh\frac{m\pi y}{a}&\\
+A_{4m}\frac{m\pi y}{a}\sinh\frac{m\pi y}{a}&,
\end{aligned}$$

$$\begin{aligned}
V_m = B_{1m}\cosh\frac{m\pi y}{a}+B_{2m}\sinh\frac{m\pi y}{a}+B_{3m}\frac{m\pi y}{a}\cosh\frac{m\pi y}{a}&\\
+B_{4m}\frac{m\pi y}{a}\sinh\frac{m\pi y}{a}&,
\end{aligned}$$

where the B_{im}'s are related to the A_{im}'s in the following manner:

$$B_{1m} = A_{2m} - \frac{3-\nu}{1+\nu} A_{3m}, \qquad B_{2m} = A_{1m} - \frac{3-\nu}{1+\nu} A_{4m},$$
$$B_{3m} = A_{4m}, \qquad B_{4m} = A_{3m}.$$

The two-dimensional elasticity problem may now be resolved into the following two edge displacement cases:

Case A. Translations Normal to Edges i and j. The boundary conditions for this case are

$$u_m = 0 \quad \text{for} \quad y = \pm \frac{b}{2}, \tag{32}$$

$$(v_m)_{y=b/2} = \bar{v}_{ijm} \sin \frac{m\pi x}{a}; \qquad (v_m)_{y=-b/2} = \bar{v}_{jim} \sin \frac{m\pi x}{a}. \tag{33}$$

The discussion can now be simplified by separation into two particular cases:

1. The symmetrical case in which $(v_m)_{y=b/2} = -(v_m)_{y=-b/2}$.
2. The anti-symmetrical case in which $(v_m)_{y=b/2} = (v_m)_{y=-b/2}$.

In the symmetrical case V_m must be an odd function of y, and hence $B_{1m} = B_{4m} = 0$. It then follows that $A_{2m} = A_{3m} = 0$.

In satisfying boundary conditions (32), we find that

$$A_{1m} = -A_{4m} \alpha_m \tanh \alpha_m \quad \text{and} \quad B_{2m} = -A_{4m} \left(\alpha_m \tanh \alpha_m + \frac{3-\nu}{1+\nu} \right)$$

and hence we now have

$$u_m = A_{4m} \left(\frac{m\pi y}{a} \sinh \frac{m\pi y}{a} - \alpha_m \tanh \alpha_m \cosh \frac{m\pi y}{a} \right) \cos \frac{m\pi x}{a}, \tag{34}$$

$$v_m = A_{4m} \left[\frac{m\pi y}{a} \cosh \frac{m\pi y}{a} - \left(\alpha_m \tanh \alpha_m + \frac{3-\nu}{1+\nu} \right) \sinh \frac{m\pi y}{a} \right] \sin \frac{m\pi x}{a}. \tag{35}$$

For the symmetrical case the displacements normal to the edges $y = \pm \frac{b}{2}$ are taken to be

$$v'_{ijm}(x) = -v'_{jim}(x) = \bar{v}'_{ijm} \sin \frac{m\pi x}{a}, \tag{36}$$

where the "primes" as before denote the symmetrical case.

From boundary conditions (33) it then follows that

$$A_{4m} = \frac{\bar{v}'_{ijm}}{\left(\alpha_m \operatorname{sech} \alpha_m - \frac{3-\nu}{1+\nu} \sinh \alpha_m \right)}.$$

Substituting this result into eqs. (34) and (35), we obtain for the symmetrical case

$$u_m = \frac{\bar{v}'_{ijm} \cos \frac{m\pi x}{a}}{\left(\alpha_m \operatorname{sech} \alpha_m - \frac{3-\nu}{1+\nu} \sinh \alpha_m\right)} \left(\frac{m\pi y}{a} \sinh \frac{m\pi y}{a} - \alpha_m \tanh \alpha_m \cosh \frac{m\pi y}{a}\right), \quad (37)$$

$$v_m = \frac{\bar{v}'_{ijm} \sin \frac{m\pi x}{a}}{\left(\alpha_m \operatorname{sech} \alpha_m - \frac{3-\nu}{1+\nu} \sinh \alpha_m\right)} \left[\frac{m\pi y}{a} \cosh \frac{m\pi y}{a} - \left(\alpha_m \tanh \alpha_m + \frac{3-\nu}{1+\nu}\right) \sinh \frac{m\pi y}{a}\right]. \quad (38)$$

In the anti-symmetrical case V_m must be an even function of y, and hence $B_{2m} = B_{3m} = 0$. It then follows that $A_{1m} = A_{4m} = 0$.

Satisfying boundary condition (32), we find that

$$A_{2m} = -A_{3m} \alpha_m \coth \alpha_m \quad \text{and} \quad B_{1m} = -A_{3m} \left(\alpha_m \coth \alpha_m + \frac{3-\nu}{1+\nu}\right).$$

Hence we now have

$$u_m = A_{3m} \left(\frac{m\pi y}{a} \cosh \frac{m\pi y}{a} - \alpha_m \coth \alpha_m \sinh \frac{m\pi y}{a}\right) \cos \frac{m\pi x}{a}, \quad (39)$$

$$v_m = A_{3m} \left[\frac{m\pi y}{a} \sinh \frac{m\pi y}{a} - \left(\alpha_m \coth \alpha_m + \frac{3-\nu}{1+\nu}\right) \cosh \frac{m\pi y}{a}\right] \sin \frac{m\pi x}{a}. \quad (40)$$

For the anti-symmetrical case the displacements normal to the edges $y = \pm \frac{b}{2}$ are as follows:

$$v''_{ijm}(x) = v''_{jim}(x) = \bar{v}''_{ijm} \sin \frac{m\pi x}{a}, \quad (41)$$

where the "double primes" as before denote the anti-symmetrical case. From boundary condition (33) we find A_{3m}. Substituting this value for A_{3m} into eqs. (39) and (40), we finally get for the anti-symmetrical case

$$u_m = -\frac{\bar{v}''_{ijm} \cos \frac{m\pi x}{a}}{\left(\alpha_m \operatorname{csch} \alpha_m + \frac{3-\nu}{1+\nu} \cosh \alpha_m\right)} \left(\frac{m\pi y}{a} \cosh \frac{m\pi y}{a} - \alpha_m \coth \alpha_m \sinh \frac{m\pi y}{a}\right), \quad (42)$$

$$v_m = -\frac{\bar{v}''_{ijm} \sin \frac{m\pi x}{a}}{\left(\alpha_m \operatorname{csch} \alpha_m + \frac{3-\nu}{1+\nu} \cosh \alpha_m\right)} \left[\frac{m\pi y}{a} \sinh \frac{m\pi y}{a} - \left(\alpha_m \coth \alpha_m + \frac{3-\nu}{1+\nu}\right) \cosh \frac{m\pi y}{a}\right]. \quad (43)$$

Since the amplitude of displacement at edge i is $\bar{v}_{ijm}$, and at edge j, $\bar{v}_{jim}$, then the symmetrical part is

$$\bar{v}'_{ijm} = \tfrac{1}{2}(\bar{v}_{ijm} - \bar{v}_{jim}) \quad (44)$$

and the anti-symmetrical part is

$$\bar{v}''_{ijm} = \tfrac{1}{2}(\bar{v}_{ijm} + \bar{v}_{jim}). \quad (45)$$

Hence adding the symmetrical and anti-symmetrical parts for u_m and v_m and using relations (44) and (45), we get for this case using the symbols at the ends of cases I A and I B.

$$\begin{aligned} u_m = \tfrac{1}{2} c_m(x)\,[\bar{v}_{ijm}\{\lambda_{5m}[S_{1m}(y)-k_{tm}C_m(y)]-\lambda_{6m}[C_{1m}(y)-k_{cm}S_m(y)]\} \\ -\bar{v}_{jim}\{\lambda_{5m}[S_{1m}(y)-k_{tm}C_m(y)]+\lambda_{6m}[C_{1m}(y)-k_{cm}S_m(y)]\}], \end{aligned} \tag{46}$$

$$\begin{aligned} v_m = \tfrac{1}{2} s_m(x)\,[\bar{v}_{ijm}\{\lambda_{5m}[C_{1m}(y)-(\mu+k_{tm})S_m(y)]-\lambda_{6m}[S_{1m}(y)-(\mu+k_{cm})C_m(y)]\} \\ -\bar{v}_{jim}\{\lambda_{5m}[C_{1m}(y)-(\mu+k_{tm})S_m(y)]+\lambda_{6m}[S_{1m}(y)-(\mu+k_{cm})C_m(y)]\}], \end{aligned} \tag{47}$$

where

$$c_m(x) = \cos\frac{m\pi x}{a}; \qquad \mu = \frac{3-\nu}{1+\nu};$$

$$\lambda_{5m} = (\alpha_m \operatorname{sech}\alpha_m - \mu\sinh\alpha_m)^{-1}; \qquad \lambda_{6m} = (\alpha_m \operatorname{csch}\alpha_m + \mu\cosh\alpha_m)^{-1}.$$

The stresses at any point in the slab can now be determined by substituting the expressions for u_m and v_m from eqs. (46) and (47) into relations (29). The forces per unit length are then obtained by multiplying the stresses by the thickness of the slab, giving the following results:

$$\begin{aligned} N_{xm} = {} & \\ D_2 s_{1m}(x)\,[\bar{v}_{ijm}\{-\lambda_{5m}[S_{1m}(y)+(\mu_4-k_{tm})C_m(y)]+\lambda_{6m}[C_{1m}(y)+(\mu_4-k_{cm})S_m(y)]\} \\ +\bar{v}_{jim}\{\ \lambda_{5m}[S_{1m}(y)+(\mu_4-k_{tm})C_m(y)]+\lambda_{6m}[C_{1m}(y)+(\mu_4-k_{cm})S_m(y)]\}], \end{aligned} \tag{48}$$

$$\begin{aligned} N_{ym} = {} & \\ D_2 s_{1m}(x)\,[\bar{v}_{ijm}\{\lambda_{5m}[S_{1m}(y)-(\mu_5+k_{tm})C_m(y)]-\lambda_{6m}[C_{1m}(y)-(\mu_5+k_{cm})S_m(y)]\} \\ -\bar{v}_{jim}\{\lambda_{5m}[S_{1m}(y)-(\mu_5+k_{tm})C_m(y)]+\lambda_{6m}[C_{1m}(y)-(\mu_5+k_{cm})S_m(y)]\}], \end{aligned} \tag{49}$$

$$\begin{aligned} N_{yxm} = {} & \\ D_2 c_{1m}(x)\,[\bar{v}_{ijm}\{\lambda_{5m}[C_{1m}(y)-(\mu_6+k_{tm})S_m(y)]-\lambda_{6m}[S_{1m}(y)-(\mu_6+k_{cm})C_m(y)]\} \\ -\bar{v}_{jim}\{\lambda_{5m}[C_{1m}(y)-(\mu_6+k_{tm})S_m(y)]+\lambda_{6m}[S_{1m}(y)-(\mu_6+k_{cm})C_m(y)]\}], \end{aligned} \tag{50}$$

where

$$D_2 = \frac{Eh}{2(1+\nu)}; \qquad \mu_4 = \frac{2\nu}{1+\nu}; \qquad \mu_5 = \frac{2}{1+\nu}; \qquad \mu_6 = \frac{1-\nu}{1+\nu}.$$

Case B. Translations Tangential to Edges i and j. The boundary conditions for this case are

$$v_m = 0 \quad \text{for} \quad y = \pm\frac{b}{2}, \tag{51}$$

$$(u_m)_{y=b/2} = \bar{u}_{im}\cos\frac{m\pi x}{a}; \qquad (u_m)_{y=-b/2} = \bar{u}_{jm}\cos\frac{m\pi x}{a}. \tag{52}$$

For simplification the solutions for u_m and v_m can again be separated into a symmetrical case and an anti-symmetrical case. The two constants for each case are determined from boundary conditions (51) and (52).

Combining the symmetrical and anti-symmetrical parts to give the complete solutions, we get for this case using the symbols at the ends of Cases I A, I B and II A.

$$u_m = \tag{53}$$
$$\tfrac{1}{2} c_m(x) \left[\bar{u}_{im}\{-\lambda_{7m}[S_{1m}(y) + (\mu - k_{cm}) C_m(y)] + \lambda_{8m}[C_{1m}(y) + (\mu - k_{tm}) S_m(y)]\} - \bar{u}_{jm}\{\ \lambda_{7m}[S_{1m}(y) + (\mu - k_{cm}) C_m(y)] + \lambda_{8m}[C_{1m}(y) + (\mu - k_{tm}) S_m(y)]\}\right],$$

$$v_m = \tfrac{1}{2} s_m(x) \left[\bar{u}_{im}\{-\lambda_{7m}[C_{1m}(y) - k_{cm} S_m(y)] + \lambda_{8m}[S_{1m}(y) - k_{tm} C_m(y)]\} - \bar{u}_{jm}\{\ \lambda_{7m}[C_{1m}(y) - k_{cm} S_m(y)] + \lambda_{8m}[S_{1m}(y) - k_{tm} C_m(y)]\}\right], \tag{54}$$

where

$$\lambda_{7m} = (\alpha_m \operatorname{csch} \alpha_m - \mu \cosh \alpha_m)^{-1}; \qquad \lambda_{8m} = (\alpha_m \operatorname{sech} \alpha_m + \mu \sinh \alpha_m)^{-1}.$$

From eqs. (53) and (54), we get the following expressions for the forces:

$$N_{xm} = \tag{55}$$
$$D_2 s_{1m}(x) \left[\bar{u}_{im}\{\lambda_{7m}[S_{1m}(y) + (\mu_7 - k_{cm}) C_m(y)] - \lambda_{8m}[C_{1m}(y) + (\mu_7 - k_{tm}) S_m(y)]\} + \bar{u}_{jm}\{\lambda_{7m}[S_{1m}(y) + (\mu_7 - k_{cm}) C_m(y)] + \lambda_{8m}[C_{1m}(y) + (\mu_7 - k_{tm}) S_m(y)]\}\right],$$

$$N_{ym} = \tag{56}$$
$$D_2 s_{1m}(x) \left[\bar{u}_{im}\{-\lambda_{7m}[S_{1m}(y) + (\mu_6 - k_{cm}) C_m(y)] + \lambda_{8m}[C_{1m}(y) + (\mu_6 - k_{tm}) S_m(y)]\} - \bar{u}_{jm}\{\ \lambda_{7m}[S_{1m}(y) + (\mu_6 - k_{cm}) C_m(y)] + \lambda_{8m}[C_{1m}(y) + (\mu_6 - k_{tm}) S_m(y)]\}\right],$$

$$N_{yxm} = \tag{57}$$
$$D_2 c_{1m}(x) \left[\bar{u}_{im}\{-\lambda_{7m}[C_{1m}(y) + (\mu_5 - k_{cm}) S_m(y)] + \lambda_{8m}[S_{1m}(y) + (\mu_5 - k_{tm}) C_m(y)]\} - \bar{u}_{jm}\{\ \lambda_{7m}[C_{1m}(y) + (\mu_5 - k_{cm}) S_m(y)] + \lambda_{8m}[S_{1m}(y) + (\mu_5 - k_{tm}) C_m(y)]\}\right],$$

where $\mu_7 = \dfrac{3+\nu}{1+\nu}$.

By superimposing the forces from the four cases given above upon those which are obtained from the fixed edge condition, the total force at any point in the slab may be obtained.

Derivation of Joint Force. Joint Displacement Equations

By evaluating the combined results of the last section for the forces at $y = \pm \frac{b}{2}$, we may obtain the expressions for the forces acting on the joint; if we observe the change in sign convention stated in Appendix A. However, instead of evaluating the quantities Q_y and M_{yx} at the joint, we evaluate the effective normal shear force [20], V_y, which is expressed as follows:

$$V_y = Q_y + \frac{\partial M_{yx}}{\partial x}.$$

It is understood that this effective shear has physical meaning only at the edges of a slab, i. e., at a joint.

If we again consider only the mth term of the Fourier series developments for the forces and displacements, we may now, from the above operations, write the joint force equations in the following form including the fixed edge forces.

$$M_{ijm} = M_{Fijm} + \frac{E h^3}{12(1-\nu^2)} \frac{m}{a} \sin\frac{m\pi x}{a} [C_1 \bar{\theta}_{im} + C_2 \bar{\theta}_{jm} - C_3 \bar{w}_{ijm} + C_4 \bar{w}_{jim}],$$

$$V_{ijm} = V_{Fijm} + \frac{E h^3}{12(1-\nu^2)} \frac{m^2}{a^2} \sin\frac{m\pi x}{a} [C_5 \bar{\theta}_{im} + C_6 \bar{\theta}_{jm} - C_7 \bar{w}_{ijm} + C_8 \bar{w}_{jim}],$$

$$N_{ijm} = N_{Fijm} + \frac{E h}{(1+\nu)^2} \frac{m}{a} \sin\frac{m\pi x}{a} [-C_9 \bar{v}_{ijm} + C_{10} \bar{v}_{jim} - C_{11} \bar{u}_{im} + C_{12} \bar{u}_{jm}],$$

$$S_{ijm} = S_{Fijm} + \frac{E h}{(1+\nu)^2} \frac{m}{a} \cos\frac{m\pi x}{a} [-C_{13} \bar{v}_{ijm} - C_{14} \bar{v}_{jim} - C_{15} \bar{u}_{im} + C_{16} \bar{u}_{jm}]$$

and

$$M_{jim} = M_{Fjim} + \frac{E h^3}{12(1-\nu^2)} \frac{m}{a} \sin\frac{m\pi x}{a} [C_1 \bar{\theta}_{jm} + C_2 \bar{\theta}_{im} + C_3 \bar{w}_{jim} - C_4 \bar{w}_{ijm}],$$

$$V_{jim} = V_{Fjim} + \frac{E h^3}{12(1-\nu^2)} \frac{m^2}{a^2} \sin\frac{m\pi x}{a} [-C_5 \bar{\theta}_{jm} - C_6 \bar{\theta}_{im} - C_7 \bar{w}_{jim} + C_8 \bar{w}_{ijm}],$$

$$N_{jim} = N_{Fjim} + \frac{E h}{(1+\nu)^2} \frac{m}{a} \sin\frac{m\pi x}{a} [-C_9 \bar{v}_{jim} + C_{10} \bar{v}_{ijm} + C_{11} \bar{u}_{jm} - C_{12} \bar{u}_{im}],$$

$$S_{jim} = S_{Fjim} + \frac{E h}{(1+\nu)^2} \frac{m}{a} \cos\frac{m\pi x}{a} [C_{13} \bar{v}_{jim} + C_{14} \bar{v}_{ijm} - C_{15} \bar{u}_{jm} + C_{16} \bar{u}_{im}],$$

where

$$C_3 = \frac{m}{a} C_3{}^*; \qquad C_4 = \frac{m}{a} C_4{}^*; \qquad C_7 = \frac{m}{a} C_7{}^*; \qquad C_8 = \frac{m}{a} C_8{}^*$$

and where

$$C_1 = \pi \left[\frac{\cosh\alpha_m}{(\alpha_m \operatorname{sech}\alpha_m + \sinh\alpha_m)} - \frac{\sinh\alpha_m}{(\alpha_m \operatorname{csch}\alpha_m - \cosh\alpha_m)}\right],$$

$$C_2 = -\pi \left[\frac{\cosh\alpha_m}{(\alpha_m \operatorname{sech}\alpha_m + \sinh\alpha_m)} + \frac{\sinh\alpha_m}{(\alpha_m \operatorname{csch}\alpha_m - \cosh\alpha_m)}\right],$$

$$C_3{}^* = C_5 = \pi^2 \left[\frac{\cosh\alpha_m}{(\alpha_m \operatorname{csch}\alpha_m + \cosh\alpha_m)} - \frac{\sinh\alpha_m}{(\alpha_m \operatorname{sech}\alpha_m - \sinh\alpha_m)} - (1-\nu)\right],$$

$$C_4{}^* = C_6 = -\pi^2 \left[\frac{\cosh\alpha_m}{(\alpha_m \operatorname{csch}\alpha_m + \cosh\alpha_m)} + \frac{\sinh\alpha_m}{(\alpha_m \operatorname{sech}\alpha_m - \sinh\alpha_m)}\right],$$

$$C_7{}^* = \pi^3 \left[\frac{\sinh\alpha_m}{(\alpha_m \operatorname{csch}\alpha_m + \cosh\alpha_m)} - \frac{\cosh\alpha_m}{(\alpha_m \operatorname{sech}\alpha_m - \sinh\alpha_m)}\right],$$

$$C_8{}^* = -\pi^3 \left[\frac{\sinh\alpha_m}{(\alpha_m \operatorname{csch}\alpha_m + \cosh\alpha_m)} + \frac{\cosh\alpha_m}{(\alpha_m \operatorname{sech}\alpha_m - \sinh\alpha_m)}\right],$$

$$C_9 = \pi \left[-\frac{\cosh\alpha_m}{\left(\alpha_m \operatorname{sech}\alpha_m - \frac{3-\nu}{1+\nu}\sinh\alpha_m\right)} + \frac{\sinh\alpha_m}{\left(\alpha_m \operatorname{csch}\alpha_m + \frac{3-\nu}{1+\nu}\cosh\alpha_m\right)}\right],$$

$$C_{10} = -\pi\left[\frac{\cosh\alpha_m}{\left(\alpha_m \operatorname{sech}\alpha_m - \frac{3-\nu}{1+\nu}\sinh\alpha_m\right)} + \frac{\sinh\alpha_m}{\left(\alpha_m \operatorname{csch}\alpha_m + \frac{3-\nu}{1+\nu}\cosh\alpha_m\right)}\right],$$

$$C_{11} = C_{13} = \pi\left[\frac{\cosh\alpha_m}{\left(\alpha_m \operatorname{csch}\alpha_m - \frac{3-\nu}{1+\nu}\cosh\alpha_m\right)} - \frac{\sinh\alpha_m}{\left(\alpha_m \operatorname{sech}\alpha_m + \frac{3-\nu}{1+\nu}\sinh\alpha_m\right)} + (1+\nu)\right],$$

$$C_{12} = C_{14} = -\pi\left[\frac{\cosh\alpha_m}{\left(\alpha_m \operatorname{csch}\alpha_m - \frac{3-\nu}{1+\nu}\cosh\alpha_m\right)} + \frac{\sinh\alpha_m}{\left(\alpha_m \operatorname{sech}\alpha_m + \frac{3-\nu}{1+\nu}\sinh\alpha_m\right)}\right],$$

$$C_{15} = \pi\left[-\frac{\sinh\alpha_m}{\left(\alpha_m \operatorname{csch}\alpha_m - \frac{3-\nu}{1+\nu}\cosh\alpha_m\right)} + \frac{\cosh\alpha_m}{\left(\alpha_m \operatorname{sech}\alpha_m + \frac{3-\nu}{1+\nu}\sinh\alpha_m\right)}\right],$$

$$C_{16} = \pi\left[\frac{\sinh\alpha_m}{\left(\alpha_m \operatorname{csch}\alpha_m - \frac{3-\nu}{1+\nu}\cosh\alpha_m\right)} + \frac{\cosh\alpha_m}{\left(\alpha_m \operatorname{sech}\alpha_m + \frac{3-\nu}{1+\nu}\sinh\alpha_m\right)}\right].$$

The directions of the corresponding joint forces and joint displacements of the two slabs meeting at a joint do not in general have a common orientation. To facilitate the writing of the joint equilibrium equations it is convenient to refer to the same set of axes for both slabs at a joint. To accomplish this purpose, we transform the displacements and forces in the (y, z) directions at each edge to the (ξ, η) directions. If we consider some joint i, with preceding joint, h, and following joint, j, then these transformations may be illustrated by figs. 3 and 4.

From fig. 3, the joint displacement transformations are

$$\begin{aligned} \bar{w}_{ijm} &= \bar{\eta}_{im}\cos\phi_{ij} - \bar{\xi}_{im}\sin\phi_{ij}, & \bar{w}_{ihm} &= \bar{\eta}_{im}\cos\phi_{ih} - \bar{\xi}_{im}\sin\phi_{ih}, \\ \bar{v}_{ijm} &= -\bar{\eta}_{im}\sin\phi_{ij} - \bar{\xi}_{im}\cos\phi_{ij}, & \bar{v}_{ihm} &= -\bar{\eta}_{im}\sin\phi_{ih} - \bar{\xi}_{im}\cos\phi_{ih}. \end{aligned}$$

From fig. 4, the joint force transformations are

$$\begin{aligned} F_{\eta ijm} &= V_{ijm}\cos\phi_{ij} - N_{ijm}\sin\phi_{ij}, & F_{\eta ihm} &= V_{ihm}\cos\phi_{ih} - N_{ihm}\sin\phi_{ih}, \\ F_{\xi ijm} &= -V_{ijm}\sin\phi_{ij} - N_{ijm}\cos\phi_{ij}. & F_{\xi ihm} &= -V_{ihm}\sin\phi_{ih} - N_{ihm}\cos\phi_{ih}. \end{aligned}$$

It is clear that the above transformations which are used in span $i-h$ also may be used in span $i-j$ at joint j.

At each joint of the folded plate structure it is only necessary to write four equilibrium equations since compatibility is automatically satisfied. Considering again some joint i, we may express the equations of equilibrium as follows:

$$\begin{aligned} M_{ijm} + M_{ihm} &= 0, \\ F_{\eta ijm} + F_{\eta ihm} &= 0, \\ F_{\xi ijm} + F_{\xi ihm} &= 0, \\ S_{ijm} + S_{ihm} &= 0. \end{aligned}$$

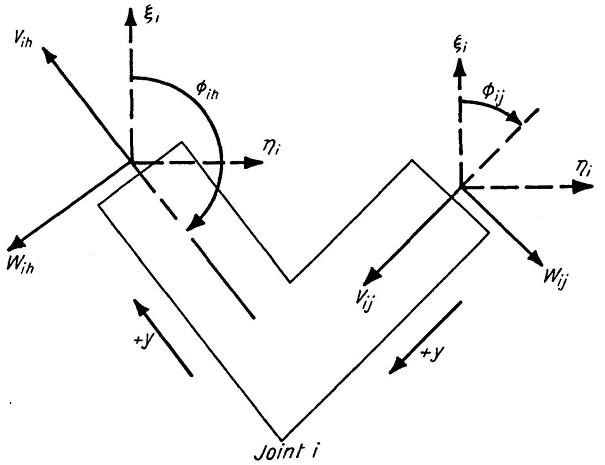

Fig. 3. Transformation of Joint Displacements.

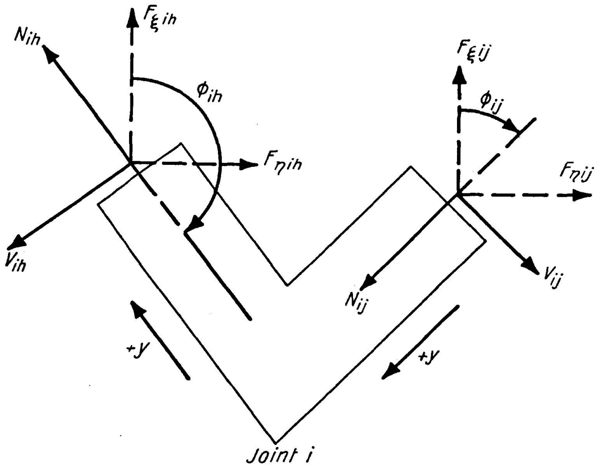

Fig. 4. Transformation of Joint Forces.

In applying the above results, the transformed displacements are substituted into the joint force equations and the transformed forces are used in the equilibrium equations as indicated above.

Boundary Equations

If we call the boundary edge or extreme edge, i, and the succeeding joint, j, then we have the following conditions for a free boundary:

$$M_{ijm} = F_{\eta\, ijm} = F_{\xi\, ijm} = S_{ijm} = 0.$$

If the boundary is fixed, then

$$\theta_{ijm} = \eta_{ijm} = \xi_{ijm} = u_{ijm} = 0.$$

If the boundary is pinned and free to slide longitudinally, then

$$\eta_{ijm} = \xi_{ijm} = 0 \quad \text{and} \quad M_{ijm} = S_{ijm} = 0.$$

If the boundary is pinned and completely restrained from sliding, then

$$\eta_{ijm} = \xi_{ijm} = u_{ijm} = 0 \quad \text{and} \quad M_{ijm} = 0.$$

For the case of an edge beam on the boundary, refer to Appendix C for the pertinent boundary equations.

Example: Three-Slab Folded Plate Structure with Fixed Boundaries

To demonstrate the use of the above equations, we solve the problem of a three-slab folded plate structure with fixed longitudinal boundaries. The cross-sectional properties of this structure and its loading are shown in fig. 5, together with the orientation of the (ξ, η) axes at each joint. The directions of these latter axes are arbitrary, although it is desirable to have one of the joint axes in the direction of one of the adjoining slabs. Hence from this chosen orientation, we have

$$\phi_{12} = \phi_{21} = -60°; \quad \phi_{23} = \phi_{32} = 0° \quad \text{and} \quad \phi_{34} = \phi_{43} = +60°.$$

Other essential properties of the structure are:

$$a = 120', \quad h = 5'' \text{ (for all slabs)}; \quad \text{and} \quad \nu = 0.2.$$

Since edges 1 and 4 are completely restrained,

$$\bar{\theta}_1 = \bar{\eta}_1 = \bar{\xi}_1 = \bar{u}_1 = \bar{\theta}_4 = \bar{\eta}_4 = \bar{\xi}_4 = \bar{u}_4 = 0.$$

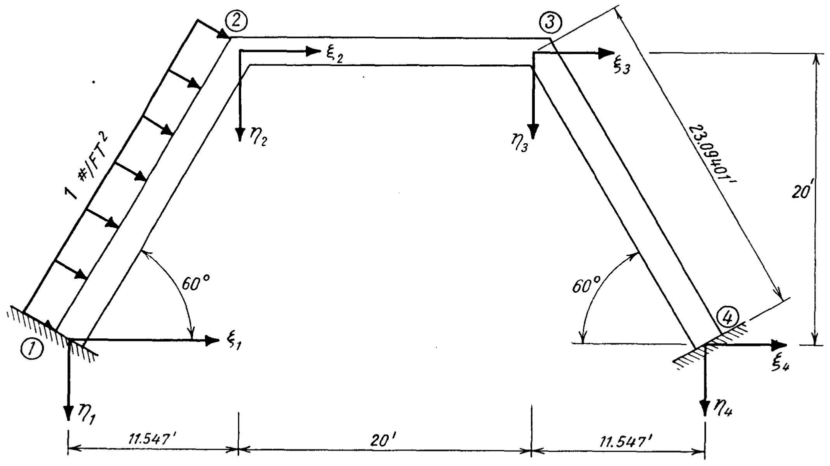

Fig. 5. Cross Section for Example.

Considering the first harmonic of the loading, or $m = 1$, we have, by definition,

$$\alpha_{12} = \alpha_{34} = 0.302300 \quad \text{and} \quad \alpha_{23} = 0.2617994,$$

where the subscripts designate the pertinent slab.

The amplitudes of the fixed edge forces for the first harmonic from Case I in Appendix B are:

$$\overline{M}_{F12} = -\overline{M}_{F21} = +55.89793; \quad \text{and} \quad \overline{V}_{F12} = \overline{V}_{F21} = +14.69943.$$

The fixed edge forces in the planes of the respective slabs (i. e., the membrane forces) are zero.

Resolving the fixed edge shears into the (ξ, η) directions, we have from the force transformation equations

$$\overline{F}_{\eta F12} = \overline{F}_{\eta F21} = +7.349715; \quad \text{and} \quad \overline{F}_{\xi F12} = \overline{F}_{\xi F21} = +12.73008.$$

In writing the joint force-displacement equations, it is convenient to change the scale of the displacements by transposing an arbitrary factor K from outside the brackets as is done in slope deflection and moment distribution analyses. This avoids extremely large stiffness coefficients and correspondingly small displacements. In the present example, since the thickness is the same for all slabs, the transposed factor is taken as:

$$K = \frac{E\,h\,\pi}{24a\,(1-\nu^2)}.$$

Using the values of α_m and the slab properties, the quantities C_1 through C_{16} for each slab are obtained and are then multiplied by the portion in front of the brackets which remains after factoring the K quantity inside.

Transforming to the (ξ, η) directions by use of the transformations given above, we obtain the following results for some typical joint forces including the fixed edge forces:

$$\overline{M}_{21} = -55.897930 + 2.353363\,\bar{\theta}_2 + 0.07650277\,\bar{\eta}_2 + 0.1325067\,\bar{\xi}_2,$$
$$\overline{M}_{23} = +2.701191\,\bar{\theta}_2 - 0.2027033\,\bar{\eta}_2 + 1.314030\,\bar{\theta}_3 + 0.2006795\,\bar{\eta}_3$$

Note that, although the same symbols are used, the displacements in the above equations are "relative" displacements, i.e., K times the true displacements.

From the joint force relations, we write the four equilibrium equations at Joint 2 and the four at Joint 3 with the following as a typical result:

$$\overline{M}_{21} + \overline{M}_{23} = 0 = -55.897930 + 5.054554\,\bar{\theta}_2 - 0.1262005\,\bar{\eta}_2 + 0.1325067\,\bar{\xi}_2 + 1.314030\,\bar{\theta}_3 + 0.2006795\,\bar{\eta}_3.$$

The eight equilibrium equations are solved for the amplitudes of the displacements using the following technique: By means of the one group of four equations, express the four displacements of Joint 3 in terms of the four displacements of Joint 2. The use of these results reduces the remaining four equations to a set involving only the four displacements of Joint 2, and these are evaluated by simultaneous solution of the four equations. The displacements of Joint 3 are then calculated by use of the first set of equations.

The extension of this technique leads to a step-wise procedure for handling systems of more than two joints without requiring, at any stage, the simultaneous solution of more than four equations.

Using this approach, we obtain for $m = 1$,

$$\begin{aligned} \bar{\theta}_2 &= +11.94895, & \bar{\theta}_3 &= -2.98351,\\ \bar{\eta}_2 &= +\ \ 5.64869, & \bar{\eta}_3 &= -5.35246,\\ \bar{\xi}_2 &= +\ \ 9.12456, & \bar{\xi}_3 &= +8.96620,\\ \bar{u}_2 &= +\ \ 1.48524, & \bar{u}_3 &= -1.49056. \end{aligned}$$

Substituting the above displacements into the force equations, we get

$$\begin{aligned} \overline{M}_{12} &= +71.071, & \overline{M}_{43} &= -\ \ 1.809,\\ \overline{F}_{\eta 12} &= +27.604, & \overline{F}_{\eta 43} &= -13.358,\\ \overline{F}_{\xi 12} &= +\ \ 3.290, & \overline{F}_{\xi 43} &= -\ \ 8.065,\\ \overline{S}_{12} &= +17.541, & \overline{S}_{43} &= -18.785. \end{aligned}$$

$$\begin{aligned} \overline{M}_{21} &= -\overline{M}_{23} = -26.137, & \overline{M}_{32} &= -\overline{M}_{34} = +\ \ 5.424,\\ \overline{F}_{\eta 21} &= -\overline{F}_{\eta 23} = -\ \ 1.600, & \overline{F}_{\eta 32} &= -\overline{F}_{\eta 34} = -\ \ 1.562,\\ \overline{F}_{\xi 21} &= -\overline{F}_{\xi 23} = +15.614, & \overline{F}_{\xi 32} &= -\overline{F}_{\xi 34} = -\ \ 1.261,\\ \overline{S}_{21} &= -\overline{S}_{23} = -28.812, & \overline{S}_{32} &= -\overline{S}_{34} = -29.418. \end{aligned}$$

By the same approach, we obtain the following results for the third harmonic, or $m=3$:

$$\begin{aligned} \bar{\theta}_2 &= +2.97037, & \bar{\theta}_3 &= -0.600974, \\ \bar{\eta}_2 &= +0.239408, & \bar{\eta}_3 &= -0.147485, \\ \bar{\xi}_2 &= +0.250406, & \bar{\xi}_3 &= +0.195773, \\ \bar{u}_2 &= +0.075439, & \bar{u}_3 &= -0.067105 \end{aligned}$$

and for the joint forces

$$\begin{aligned} \bar{M}_{12} &= +19.848, & \bar{M}_{43} &= -0.5685, \\ \bar{F}_{\eta 12} &= +\ 5.321, & \bar{F}_{\eta 43} &= +0.1641, \\ \bar{F}_{\xi 12} &= +\ 3.063, & \bar{F}_{\xi 43} &= -1.3180, \\ \bar{S}_{12} &= -\ 0.7429, & \bar{S}_{43} &= -0.8648. \end{aligned}$$

$$\begin{aligned} \bar{M}_{21} &= -\bar{M}_{23} = -8.382, & \bar{M}_{32} &= -\bar{M}_{34} = +1.642, \\ \bar{F}_{\eta 21} &= -\bar{F}_{\eta 23} = -0.5777, & \bar{F}_{\eta 32} &= -\bar{F}_{\eta 34} = -0.4646, \\ \bar{F}_{\xi 21} &= -\bar{F}_{\xi 23} = +5.245, & \bar{F}_{\xi 32} &= -\bar{F}_{\xi 34} = -0.3956, \\ \bar{S}_{21} &= -\bar{S}_{23} = -2.115, & \bar{S}_{32} &= -\bar{S}_{34} = -2.463. \end{aligned}$$

For the fifth harmonic, or $m=5$, we obtain the following results:

$$\begin{aligned} \bar{\theta}_2 &= +1.08334, & \bar{\theta}_3 &= -0.138661, \\ \bar{\eta}_2 &= +0.0695769, & \bar{\eta}_3 &= -0.0232892, \\ \bar{\xi}_2 &= +0.0565577, & \bar{\xi}_3 &= +0.0259520, \\ \bar{u}_2 &= +0.0187552, & \bar{u}_3 &= -0.0110577 \end{aligned}$$

and the joint forces are

$$\begin{aligned} \bar{M}_{12} &= +8.924, & \bar{M}_{43} &= -0.09978, \\ \bar{F}_{\eta 12} &= +2.020, & \bar{F}_{\eta 43} &= -0.1720, \\ \bar{F}_{\xi 12} &= +2.168, & \bar{F}_{\xi 43} &= -0.1218, \\ \bar{S}_{12} &= -0.3201, & \bar{S}_{43} &= +0.08602. \end{aligned}$$

$$\begin{aligned} \bar{M}_{21} &= -\bar{M}_{23} = -4.046, & \bar{M}_{32} &= -\bar{M}_{34} = +0.5039, \\ \bar{F}_{\eta 21} &= -\bar{F}_{\eta 23} = -0.3462, & \bar{F}_{\eta 32} &= -\bar{F}_{\eta 34} = -0.1687, \\ \bar{F}_{\xi 21} &= -\bar{F}_{\xi 23} = +2.946, & \bar{F}_{\xi 32} &= -\bar{F}_{\xi 34} = -0.1454, \\ \bar{S}_{21} &= -\bar{S}_{23} = -0.4555, & \bar{S}_{32} &= -\bar{S}_{34} = -0.5754. \end{aligned}$$

It can be seen that the above results have converged sufficiently for most practical purposes, but for greater accuracy more harmonics should be taken. The above harmonics may now be combined, if it is remembered that each of the above results is to be multiplied by $\sin\frac{m\pi x}{a}$, except $\bar{u}$ and $\bar{S}$, which are multiplied by $\cos\frac{m\pi x}{a}$.

The forces at any point in the structure now may be obtained from the above results in conjunction with the edge displacement-force relations and fixed edge force expressions for interior points.

Since this particular example was used to demonstrate a general procedure of solution for a folded plate structure, advantage was not taken of the symmetry of the cross-section of this structure. Because of this symmetry, this example could have been resolved into a symmetrical part and an anti-symmetrical part with a resulting saving in labor.

It has been found by the authors that the effect of Poisson's ratio is quite significant, and the arbitrary use of $\nu = 0$ generally is not justified. Examples worked by the authors using $\nu = 0.2$ and $\nu = 0$ showed discrepancies as large as 33 per cent for the joint forces, and differences beyond comparison for certain interior slab forces.

General Procedure of Solution

In view of the Example (p. 73), we are now in a position to suggest a general method for solving the basic folded plate structure:

1. Locate the (ξ, η) coordinate axes at the boundaries and at each joint so that at each location one of the axes is in the direction of one of the slabs. (This reduces the amount of coupling between displacements.)

2. Starting with the first harmonic ($m = 1$), calculate the fixed edge forces (using the pertinent equations of Appendix B) and resolve these forces into the joint coordinate directions defined in Step 1.

3. Calculate the quantities C_1 through C_{16} for each slab by using the equations given in the text.

4. From the joint force equations, factor a common quantity from the outside of the brackets to the inside and combine this quantity with the unknown displacements. (This combination we call the "relative" displacement, as indicated in the Example.)

5. Multiply each C_i by the quantity remaining outside the brackets.

6. Transform the displacements and forces at each joint to the (ξ, η) directions by use of the transformation equations given in the text.

7. Using the joint force equations, write the boundary and joint equilibrium equations.

8. Solve the simultaneous equations of Step 7 for the unknown relative displacements. (It is preferable to solve these equations in blocks of four, as indicated in the Example.)

9. Calculate the joint forces by substituting the values of the "relative" displacements into the joint force equations. (The forces at any interior point may now be calculated by substituting the appropriate joint displacements into the edge displacement-force relations and adding any forces arising from the fixed edge condition.)

10. Repeat the above steps for the second harmonic and any additional harmonics until the desired degree of convergence is attained.

11. Combine the corresponding results from each harmonic to obtain the final values for the desired displacements and internal forces.

Bibliography

1. EHLERS, G., «Ein neues Konstruktionsprinzip», Bauingenieur, Vol. 9, 1930, p. 125.
2. CRAEMER, H., «Theorie der Faltwerke», Beton und Eisen, Vol. 29, 1930, p. 276.
3. EHLERS, G., «Die Spannungsermittlung in Flächentragwerken», Beton und Eisen, Vol. 29, 1930, p. 281.
4. GRUBER, E., «Berechnung prismatischer Scheibenwerke», Intern. Assoc. Bridge and Struct. Engg., Memoires, Vol. 1, 1932, p. 225.
5. GRUENING, G., «Die Nebenspannungen der prismatischen Faltwerke», Ingenieur-Archiv, Vol. 3, Nr. 4, 1932.
6. GOLDENBLATT, J. and RATZ, E., «Berechnung von Faltwerken, welche aus Scheiben mit verschiedenen statischen Systemen bestehen», Beton und Eisen, Vol. 33, 1934, p. 369.
7. GRUBER, E., «Die Berechnung pyramidenartiger Scheibenwerke und ihre Anwendung auf Kaminkühler», Intern. Assoc. Bridge and Struct. Engg., Memoires, Vol. 2, 1933/34, p. 206.
8. FLÜGGE, W., «Statik und Dynamik der Schalen», Julius Springer, Publisher, Berlin, 1934, p. 174.
9. GRUBER, E., «Die Berechnung äußerlich statisch unbestimmter prismatischer Scheibenwerke», Intern. Assoc. Bridge and Struct. Engg., Memoires, Vol. 3, 1935, p. 134.
10. OHLIG, R., «Beitrag zur Theorie der prismatischen Faltwerke», Ingenieur-Archiv, Vol. 6, Nr. 5, 1935, p. 346.
11. CRAEMER, H., «Der heutige Stand der Theorie der Scheibenträger und Faltwerke in Eisenbeton», Beton und Eisen, Vol. 36, 1937, pp. 264 and 297.
12. CRAEMER, H., «Die Beanspruchung von Faltwerken mit gedrungenen Einzelscheiben», Bauingenieur, Sept. 1940, p. 268.
13. GRUBER, E., «Hohlträger als Faltwerke», Intern. Assoc. Bridge and Struct. Engg., Memoires, Vol. 7, 1943/44, p. 139.
14. WINTER, G. and PEI, M., "Hipped Plate Construction", Journal of the A.C.I., Vol. 18, No. 5, Jan. 1947.
15. GRUBER, E., «Die durchlaufenden, prismatischen Faltwerke», Intern. Assoc. Bridge and Struct. Engg., Memoires, Vol. 12, 1952, p. 167.
16. CRAEMER, H., "Design of Prismatic Shells", Journal of the A.C.I., Vol. 24, No. 6, Feb. 1953.
17. GAAFAR, I., "Hipped Plate Analysis, Considering Joint Displacements", A.S.C.E. Transactions, Vol. 119, 1954, p. 743.
18. GRUBER, E., «*Die genaue Membranentheorie der prismatischen Faltwerke*», Intern. Assoc. Bridge and Struct. Engg., Memoires, Vol. 11, 1951, p. 129.
19. WERFEL, A., «Die genaue Theorie der prismatischen Faltwerke und ihre praktische Anwendung», Intern. Assoc. Bridge and Struct. Engg., Memoires, Vol. 14, 1954, p. 277.
20. TIMOSHENKO, S., Theory of Plates and Shells, McGraw-Hill Book Company, New York, 1940.
21. TIMOSHENKO, S. and GOODIER, J. N., Theory of Elasticity, McGraw-Hill Book Co., New York, 1951.

Appendix A. Notation and Sign Convention

The symbols which are not defined in the text are as follows:

a, b, h = longitudinal, transverse, and thickness dimensions of a slab, respectively.

E, G, ν = modulus of elasticity, shearing modulus of elasticity, and Poisson's ratio, respectively.

D = $\frac{E h^3}{12(1-\nu^2)}$; modulus of rigidity.

x, y, z = rectangular coordinate axes for slab.

u, v, w = displacements in the x, y, z directions, respectively, for any point in the mid-plane of the slab.

u_i, v_{ij}, w_{ij} = u, v, w displacements along edge i of slab $i-j$.

θ_i = rotational displacement about edge i of the tangent to slab $i-j$.

(M_x, M_y); (M_{xy}, M_{yx}); (Q_x, Q_y); (N_x, N_y); (N_{xy}, N_{yx}); = internal slab forces per unit length in the coordinate directions, respectively, in pairs: bending moments, twisting moments, plate shear forces, membrane forces, and membrane shearing forces.
(For an illustration of these forces see figs. 7 and 8.)

V_y = $Q_y + \frac{\partial M_{yx}}{\partial x}$; effective normal shear force.

$\sigma_x, \sigma_y, \tau_{xy}$ = $\frac{N_x}{h}$, $\frac{N_y}{h}$, and $\frac{N_{xy}}{h}$, respectively.

m = number of the harmonic or number of half-waves in the x-direction.

α_m = $\frac{m \pi b}{2a}$, coefficient parameter.

M_{ij}, S_{ij}, N_{ij}, V_{ij} = joint forces per unit length acting at joint i in span $i-j$, respectively, the joint bending moment and the joint forces in the x, y, and z directions.

ξ, η = orthogonal displacements in the plane of the cross-section.

$F_{\xi ij}, F_{\eta ij}$ = joint forces per unit length acting at joint i in span $i-j$ in the ξ and η directions, respectively.

ϕ_{ij} = angle of transformation from the (y, z) system to the (ξ, η) system at joint i for span $i-j$.

t = thickness of edge beam.

d = depth of edge beam.

The mth term of the Fourier series developments for any of the forces and displacements given above is denoted by the letter "m", in the subscript.

The amplitude or maximum value for a particular harmonic of any of the above forces and displacements is designated by a "bar" over the symbol.

The fixed edge forces and the internal forces arising from the fixed edge condition are designated by the letter "F" in the subscript.

The location of the coordinate axes for the individual slab is as shown in fig. 6. The z-axis completes the right hand triad (x, y, z). Fig. 6 also shows that the edges, $y = +\frac{b}{2}$, and $y = -\frac{b}{2}$, are designated "i" and "j" respectively.

Positive displacements of u, v, and w are taken in the positive x, y, and z directions, respectively.

The positive directions for the internal slab forces are shown in figs. 7 and 8.

For convenience, we always consider the structure as running from left to right longitudinally with the observer always facing toward the left end. The origin of coordinates is located at the left end with the positive longitudinal axis (x-axis) directed toward the observer. The y-axis for a particular slab is oriented so that its positive direction is always toward the preceding joint. The orientation of axes for a complete structure is shown in fig. 9. The slab coordinate axes (x, y, z) also pertain to the joints which bound the slab.

Fig. 9 also shows that the joints preceding and following a particular slab

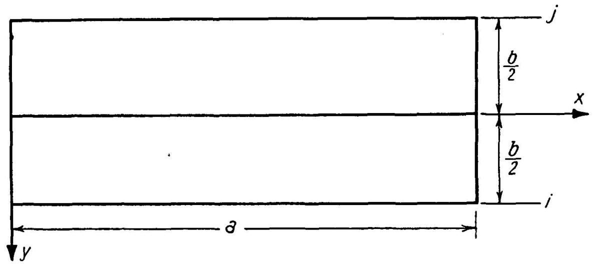

Fig. 6. Slab Coordinate System.

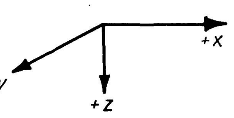

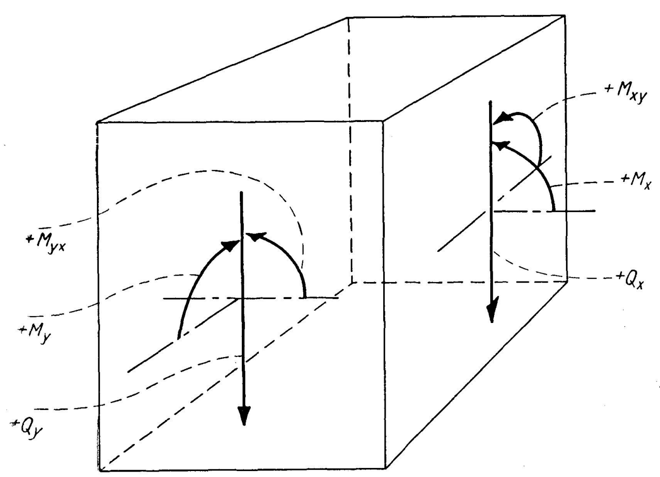

Fig. 7. Internal Forces due to Plate Action.

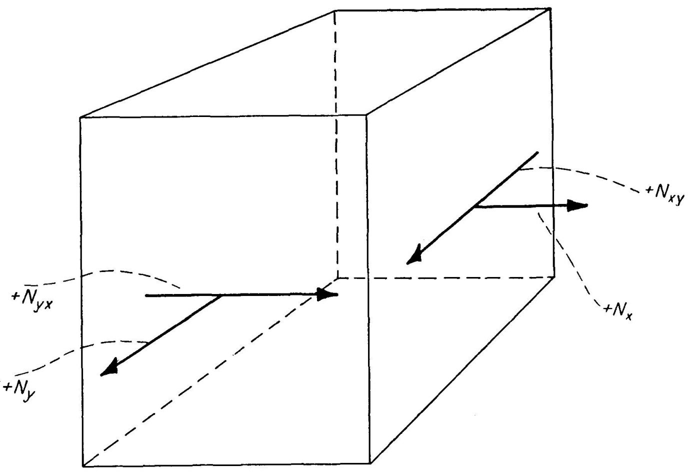

Fig. 8. Internal Forces due to Membrane Action.

are designated "i" and "j", respectively in accordance with the edge designation for the individual slab given above.

A counter-clockwise rotation of the joint, as seen looking toward the left end, and joint displacements in the positive coordinate directions, are taken as positive.

A clockwise joint moment and joint forces acting in the positive coordinate directions are taken as positive.

The joint sign convention differs from that for the individual slab only in the sign of the forces acting at the joint edge corresponding to $y = +\frac{b}{2}$ (or edge i). The signs of the forces acting at the joint edge corresponding to $y = -\frac{b}{2}$ (or edge j) and the signs of the displacements are the same for the two systems.

The (ξ, η, x) axes are orthogonal and form a left hand triad. The angle ϕ is taken as positive if measured clockwise from the positive ξ-direction to the negative y-direction. (See figs. 3, 4.)

For the fixed edge forces, a positive load is considered as acting in the positive coordinate directions of the slab.

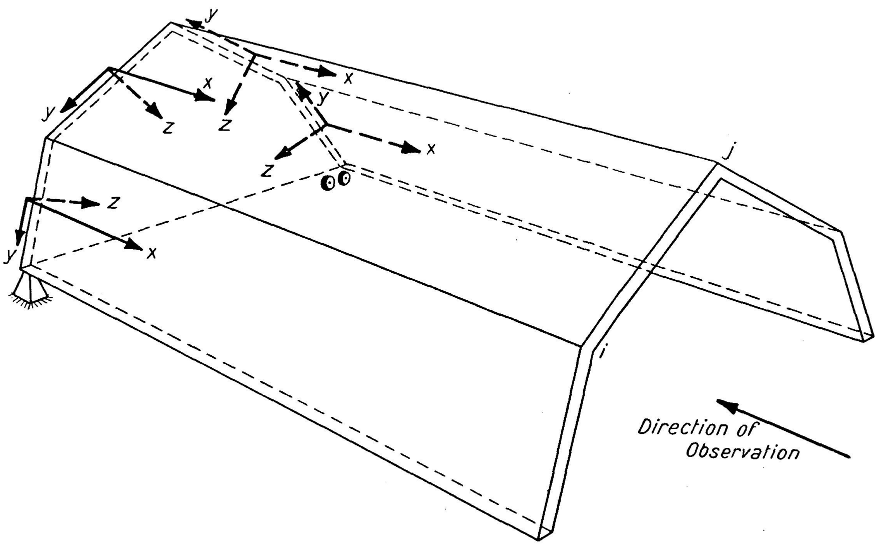

Fig. 9. Orientation of Axes for Folded Plate Structure.

Appendix B. Fixed Edge Forces

Joint forces arise due to two effects: (1) the rotations and translations of the joints, and (2) the loading. The joint forces due to the joint displacements have been fully developed and it is the purpose of this section to find the joint forces due to various types of loading.

The Fixed Edge Forces are the forces due to loading which would exist at the longitudinal edges of a slab if these edges were constrained against all displacement. The total edge forces are obtained by superimposing upon the fixed edge forces the additional forces due to the edge displacements. As in the other sections of this paper, the transverse edges ($x=0, a$) are assumed to be completely restrained in the planes of the end diaphragms and to have no restraints normal to those planes.

The fixed edge forces are given below for the important cases of uniform normal load and uniform load in the y-direction. The fixed edge forces for the general case of normal loading and for the general case of loading in the plane of the slab also have been determined by the authors, but, for brevity are not presented here.

The following procedure is suggested for determining the fixed edge forces for any case. The loading is first expanded into a Fourier sine series, using a single series if the load does not vary in the y-direction, otherwise using a double sine series. Displacements are then assumed in a similar series form and the coefficients are determined by substitution of the assumed series into the appropriate differential equations. In general, these particular solutions do not satisfy the geometrical boundary conditions and it is necessary to superimpose solutions of the homogeneous differential equations to nullify the untenable displacements associated with the particular solution.

Using the above approach, the fixed edge forces and associated internal forces have been found for the following cases:

Case I. Uniform Load Normal to the Slab

If q is the intensity of the uniform normal load, then the fixed edge forces for the mth harmonic are ($m=1,3,5\ldots$):

$$M_{Fijm} = -M_{Fjim} = \frac{4\,q\,a^2}{m^3\pi^3}\left[\frac{2\cosh\alpha_m}{(\alpha_m\operatorname{csch}\alpha_m+\cosh\alpha_m)}-1\right]\sin\frac{m\pi x}{a},$$

$$V_{Fijm} = V_{Fjim} = \frac{8\,q\,a}{m^2\pi^2}\,\frac{\sinh\alpha_m}{(\alpha_m\operatorname{csch}\alpha_m+\cosh\alpha_m)}\sin\frac{m\pi x}{a}.$$

The resulting internal forces for this case are

$$M_{yFm} = -\frac{4\,q\,a^2(1-\nu)}{m^3\pi^3}\sin\frac{m\pi x}{a}\cdot\left\{\frac{\left[\frac{m\pi y}{a}\sinh\frac{m\pi y}{a}+\left(\frac{1+\nu}{1-\nu}-\alpha_m\coth\alpha_m\right)\cosh\frac{m\pi y}{a}\right]}{(\alpha_m\operatorname{csch}\alpha_m+\cosh\alpha_m)}-\frac{\nu}{1-\nu}\right\},$$

$$M_{xFm} = \frac{4\,q\,a^2(1-\nu)}{m^3\pi^3}\sin\frac{m\pi x}{a}\cdot\left\{\frac{\left[\frac{m\pi y}{a}\sinh\frac{m\pi y}{a}-\left(\frac{1+\nu}{1-\nu}+\alpha_m\coth\alpha_m\right)\cosh\frac{m\pi y}{a}\right]}{(\alpha_m\operatorname{csch}\alpha_m+\cosh\alpha_m)}+\frac{1}{1-\nu}\right\},$$

$$Q_{yFm} = -\frac{8\,q\,a}{m^2\pi^2}\,\frac{\sinh\frac{m\pi y}{a}}{(\alpha_m\operatorname{csch}\alpha_m+\cosh\alpha_m)}\sin\frac{m\pi x}{a},$$

$$Q_{xFm} = -\frac{4qa}{m^2\pi^2}\cos\frac{m\pi x}{a}\left[\frac{2\cosh\frac{m\pi y}{a}}{(\alpha_m \operatorname{csch}\alpha_m + \cosh\alpha_m)} - 1\right],$$

$$M_{yxFm} = -M_{xyFm} = -\frac{4qa^2(1-\nu)}{m^3\pi^3}\frac{\cos\frac{m\pi x}{a}}{(\alpha_m \operatorname{csch}\alpha_m + \cosh\alpha_m)} \cdot \left[\frac{m\pi y}{a}\cosh\frac{m\pi y}{a} - \alpha_m \coth\alpha_m \sinh\frac{m\pi y}{a}\right].$$

Case II. Uniform Load in the Plane of the Slab Acting in the $+y$-Direction

If p is the intensity of the uniform load in the plane of the slab, then the fixed edge forces for the mth harmonic are ($m = 1, 3, 5, \ldots$):

$$N_{Fijm} = N_{Fjim} = \frac{16hap}{(1+\nu)m^2\pi^2}\frac{\sinh\alpha_m}{\left(\alpha_m \operatorname{csch}\alpha_m + \frac{3-\nu}{1+\nu}\cosh\alpha_m\right)}\sin\frac{m\pi x}{a},$$

$$S_{Fijm} = -S_{Fjim} = -\frac{4hap}{(1+\nu)m^2\pi^2}\left[\frac{4\cosh\alpha_m}{\left(\alpha_m \operatorname{csch}\alpha_m + \frac{3-\nu}{1+\nu}\cosh\alpha_m\right)} - (1+\nu)\right]\cos\frac{m\pi x}{a}.$$

The resulting internal forces for this case are

$$N_{yFm} = \frac{8hap}{m^2\pi^2}\frac{\sin\frac{m\pi x}{a}}{\left(\alpha_m \operatorname{csch}\alpha_m + \frac{3-\nu}{1+\nu}\cosh\alpha_m\right)}\left[\frac{m\pi y}{a}\cosh\frac{m\pi y}{a} - \left(\alpha_m\coth\alpha_m + \frac{2}{1+\nu}\right)\sinh\frac{m\pi y}{a}\right],$$

$$N_{xFm} = -\frac{8hap}{m^2\pi^2}\frac{\sin\frac{m\pi x}{a}}{\left(\alpha_m \operatorname{csch}\alpha_m + \frac{3-\nu}{1+\nu}\cosh\alpha_m\right)}\left[\frac{m\pi y}{a}\cosh\frac{m\pi y}{a} - \left(\alpha_m\coth\alpha_m - \frac{2\nu}{1+\nu}\right)\sinh\frac{m\pi y}{a}\right],$$

$$N_{xyFm} = N_{yxFm} = \frac{4hap}{m^2\pi^2}\cos\frac{m\pi x}{a} \cdot \left\{\frac{2\left[\frac{m\pi y}{a}\sinh\frac{m\pi y}{a} - \left(\alpha_m\coth\alpha_m + \frac{1-\nu}{1+\nu}\right)\cosh\frac{m\pi y}{a}\right]}{\left(\alpha_m \operatorname{csch}\alpha_m + \frac{3-\nu}{1+\nu}\cosh\alpha_m\right)} + 1\right\}.$$

Appendix C. Joint Force-Displacement Equations for an Edge Beam

Many folded plate structures utilize edge beams on their longitudinal boundaries and it is the purpose of this section to present the joint equations for the edge beam in forms similar to those for the slab.

The edge beam to be considered is of rectangular cross section and is attached to the neighboring slab along the centerline of one of its faces with the opposite face free. The end $x=0$ and $x=a$, as with the slabs, are not permitted to have displacements in the planes of the end diaphragms, but have no restraint normal to these planes. In particular, the ends are simply supported with respect to bending and restrained from twisting, but with no restraint against warping. The orientation of the (x, y, z) axes follows the same rule as for the slabs (see fig. 10), and therefore either edge "i" or edge "j" may be the contacting edge. Hence we must give joint equations for these two possibilities.

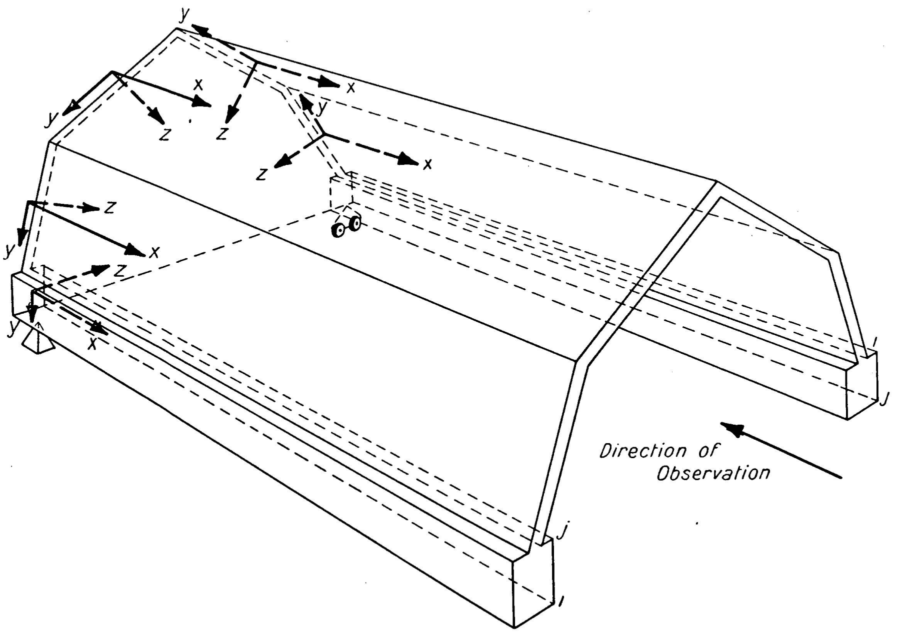

Fig. 10. Orientation of Axes for Folded Plate Structure with Edge Beams.

An approach to this problem can be made by first giving displacements to the contacting edge of the same type as those for the slab. These edge displacements can then be related to the internal restraining forces by use of elastic deformation theory. Writing the equilibrium equations for a differential element along the length of the beam will relate the internal restraining forces to the edge forces. Hence the edge forces may be related to the edge displacements through a set of differential equations. The required joint force-joint displacement equations can now be obtained by taking consistent Fourier series developments for the edge displacements and edge forces. This latter step relates the joint forces to the joint displacements by a system of linear algebraic equations similar to those for the slab. If we first consider edge "i" to be the contacting edge, then these last relations may be written as follows:

$$M_{ijm} = \frac{E\,t^3\,d}{48\,k_1}\,\frac{m^2\pi^2}{a^2}\sin\frac{m\pi x}{a}\left\{\left[16\,\frac{G}{E}\left(1-0.630\,\frac{t}{d}\right)k_1+\frac{m^2\pi^2}{a^2}d^2\right]\bar{\theta}_{im} - 2\,d\,\frac{m^2\pi^2}{a^2}\,\overline{w}_{ijm}\right\},\text{[1]}$$

[1]) These equations are valid for $d \geqq t$.

$$V_{ijm} = \frac{E\,t^3\,d}{24\,k_1}\,\frac{m^4\pi^4}{a^4}\sin\frac{m\pi x}{a}\,[d\,\bar{\theta}_{im} - 2\,\bar{w}_{ijm}],$$

$$N_{ijm} = -\frac{E\,t\,d^2}{6\,k_2}\,\frac{m^3\pi^3}{a^3}\sin\frac{m\pi x}{a}\left[2\,d\frac{m\pi}{a}\bar{v}_{ijm} + 3\,\bar{u}_{im}\right],$$

$$S_{ijm} = -\frac{E\,t\,d}{2\,k_2}\,\frac{m^2\pi^2}{a^2}\cos\frac{m\pi x}{a}\left[d\,\frac{m\pi}{a}\bar{v}_{ijm} + 2\,k_3\,\bar{u}_{im}\right],$$

where

$$k_1 = \left(1 + \frac{E\,t^2}{10\,G}\,\frac{m^2\pi^2}{a^2}\right); \quad k_2 = \left(1 + \frac{2\,E\,d^2}{5\,G}\,\frac{m^2\pi^2}{a^2}\right), \quad \text{and} \quad k_3 = \left(1 + \frac{E\,d^2}{10\,G}\,\frac{m^2\pi^2}{a^2}\right).$$

If edge "j" is the contacting edge, then

$$M_{jim} = \frac{E\,t^3\,d}{48\,k_1}\,\frac{m^2\pi^2}{a^2}\sin\frac{m\pi x}{a}\left\{\left[16\frac{G}{E}\left(1 - 0.630\frac{t}{d}\right)k_1 + \frac{m^2\pi^2}{a^2}d^2\right]\bar{\theta}_{jm} + 2\,d\frac{m^2\pi^2}{a^2}\bar{w}_{jim}\right\},^{1)}$$

$$V_{jim} = -\frac{E\,t^3\,d}{24\,k_1}\,\frac{m^4\pi^4}{a^4}\sin\frac{m\pi x}{a}\,[d\,\bar{\theta}_{jm} + 2\,\bar{w}_{jim}],$$

$$N_{jim} = \frac{E\,t\,d^2}{6\,k_2}\,\frac{m^3\pi^3}{a^3}\sin\frac{m\pi x}{a}\left[-2\,d\frac{m\pi}{a}\bar{v}_{jim} + 3\,\bar{u}_{jm}\right],$$

$$S_{jim} = \frac{E\,t\,d}{2\,k_2}\,\frac{m^2\pi^2}{a^2}\cos\frac{m\pi x}{a}\left[d\frac{m\pi}{a}\bar{v}_{jim} - 2\,k_3\,\bar{u}_{jm}\right].$$

Following the same transformation rule for the edge beam as for the slab, the equilibrium equations for a joint formed by an edge beam and a slab are of the same form as those for a joint formed by two slabs. Hence if we call the edge beam joint j, and the following joint k, with the free edge designated i, we may write the following set of equilibrium equations for joint j:

$$\begin{aligned} M_{jkm} + M_{jim} &= 0, \\ F_{\eta jkm} + F_{\eta jim} &= 0, \\ F_{\xi jkm} + F_{\xi jim} &= 0, \\ S_{jkm} + S_{jim} &= 0. \end{aligned}$$

Summary

This paper develops a procedure for analyzing folded plate structures which considers both plate and membrane action. Equations are derived which relate each joint force to a linear combination of the joint displacements. In this manner compatibility is automatically satisfied at each joint, and it is only necessary to write $4n$ equilibrium equations, where n is the number of joints with unknown forces and displacements, for each harmonic of the Fourier expansion.

Joint forces due to common loading conditions are given as well as joint equations for a rectangular edge beam.

The application of the theory is illustrated by the analysis of a three-slab folded plate structure with fixed boundaries.

Résumé

Les auteurs exposent une méthode de calcul des systèmes de parois prismatiques qui tient compte aussi bien de l'effet de plaque que de l'effet de membrane. Ils établissent des équations qui rapportent chaque contrainte d'arête à une combinaison linéaire de déformations d'arête. Les conditions de compatibilité sont ainsi automatiquement satisfaites pour chaque arête et il suffit d'écrire $4n$ conditions d'équilibre pour chaque terme du développement en série de Fourier, n désignant le nombre des arêtes impliquant des contraintes et des déformations non connues. Les auteurs indiquent des valeurs de contraintes d'arête résultant de charges courantes, ainsi que des équations d'arête pour une poutre de retombée rectangulaire.

L'application de la théorie est illustrée par le calcul d'un système prismatique à trois parois avec bords fixes.

Zusammenfassung

In dieser Abhandlung wird ein Verfahren zur Berechnung von Faltwerken entwickelt, welches sowohl die Platten- wie die Membranwirkung berücksichtigt. Es werden Gleichungen abgeleitet, welche jede Kantenkraft auf eine lineare Kombination der Kantenverschiebungen beziehen. Auf diese Weise werden die Verträglichkeitsbedingungen automatisch in jeder Kante erfüllt, und es ist nur noch nötig, $4n$ Gleichgewichtsbedingungen für jedes Glied der Fourierentwicklung anzuschreiben, wobei n die Zahl der Kanten mit unbekannten Kräften und Verschiebungen bedeutet. Es werden sowohl Kantenkräfte infolge gewöhnlicher Belastungen als auch Kantengleichungen für einen rechteckigen Randbalken angegeben.

Die Anwendung der Theorie wird durch die Berechnung eines Drei-Platten-Faltwerkes mit festen Rändern illustriert.